Bioorganic & Medicinal Chemistry 18 (2010) 3252–3260

Contents lists available at ScienceDirect

Bioorganic & Medicinal Chemistry

journal homepage: www.elsevier.com/locate/bmc

Synthesis and biological activity of cyclotetrapeptide analogues of the natural HDAC inhibitor FR235222

Stefania Terracciano [a], Simone Di Micco [a], Giuseppe Bifulco [a], Paola Gallinari [b], Raffaele Riccio [a], Ines Bruno [a,*]

[a] Dipartimento di Scienze Farmaceutiche, Università degli Studi di Salerno, Via Ponte Don Melillo, 84084 Fisciano (SA), Italy
[b] Dipartimento di Oncologia, Istituto di Ricerche di Biologia Molecolare P. Angeletti, 00040 Pomezia, Roma, Italy

ARTICLE INFO

Article history:
Received 21 December 2009
Revised 8 March 2010
Accepted 11 March 2010
Available online 15 March 2010

Keywords:
Anticancer drugs
Cyclopeptides
HDAC
Olefin metathesis
Molecular docking

ABSTRACT

In the course of our ongoing efforts to discover new and more effective HDAC inhibitors useful for the development of promising anticancer candidates, we have recently undertaken a molecular modelling study on a small collection of FR235222 analogues, synthesized by us in the frame of a structure–activity relationship investigation, made in order to identify the key structural elements essential for the activity. Progress made in structure elucidation of HDAC active site, together with accurate docking calculations, provided new structural insights useful for a further refinement of the tetrapeptide scaffold which should assure an optimal interaction between the synthetic ligands and the biological target. Following the computer aided suggestions we synthesized six new cyclotetrapeptide analogues of the lead compound (**3**–**8**), bearing a carboxylic or an hydroxamic acid functionality as Zn binding moiety. Herein we describe their synthesis and their inhibition activity on different HDAC isoforms.

1. Introduction

The posttranslational modification of histone core, known as epigenetic mechanism, is fundamentally important to conformational changes of the chromatin and to the modulation of transcriptional events.[1] In particular the level of acetylation of histone tails, which are controlled by two counteracting enzyme families, HATs and HDACs, plays a crucial role in the regulation of transcriptional machinery to switch the activity of genes involved in cellular proliferation on and off.[2] In the last years HDAC inhibitors have emerged as precious tools in cancer chemoprevention as they showed to induce growth arrest, differentiation, and/or apoptotic cell death.[3] Although many details of their mechanism of action have been disclosed, several basic aspects are not fully understood also because besides histones, the key substrates, HDACs seem to regulate the functions of a growing list of non histone proteins such as the oncosuppressor p53, transcription factors, HSP90 and several nuclear importers;[4] for that reason, clarifying the exact mechanism of HDAC inhibitors anticancer effects in such a complex network of cellular signalling is not a simple task. Another topic that still needs to be accomplished is to identify the precise role played in tumorogenesis by the individual HDAC isoforms. HDACs, in fact, can be divided into four groups: classes I, II and IV are all Zn-dependent enzymes showing relevant sequence similarity in their catalytic site which is represented by a long and narrow channel with the Zn ion localized at the bottom; in contrast, class III, also named sirtuins, show different structural features, are NAD^+-dependent deacetylase and are not considered 'classical' HDACs.[3c,4,5] Concerning their localization in cellular framework, class I and IV are basically nuclear proteins whereas class II HDACs shuttle between the nucleus and the cytoplasm.[3c,4,5] Despite the intense research in this area unfortunately very selective HDACi have not been yet identified so far as a consequence of the limited structural information available, therefore the discovery of small molecules able to selectively perturb th e individual HDAC isoforms would be extremely useful to help clarify several mechanistic details.

2. Discussion

Recently we had the occasion to explore the chemical and the pharmacological properties of FR235222,[6] a natural product isolated from the fermentation broth of a fungus, *Acremonium* sp. and possessing a potent HDAC inhibition activity. This metabolite belongs to cyclopeptide class of HDAC inhibitors which includes,

Abbreviations: Boc, *tert*-butyloxycarbonyl; ClTrt-Cl, 2-chlorotrityl chloride-resin; DIEA, *N*,*N*-diisopropylethylamine; DCM, dichloromethane; DMF, *N*,*N*-dimethylformamide; Fmoc, 9-fluorenylmethyloxycarbonyl; Fmoc-L-AllylGly-OH, *N*-α-Fmoc-L-allyliglycine; Fmoc-Gly-OH, *N*-α-Fmoc-glycine; Fmoc-D-Pro-OH, *N*-α-Fmoc-proline; Fmoc-D-Trp(Boc)-OH, *N*-α-Fmoc-N^{in}-Boc-D-tryptophan; HATU, *N*-[(dimethylamino)-1*H*-1,2,3-triazolo-[4,5-*b*]pyridin-1-yl-methylene]-*N*-methyl-methanaminium hexafluoroposphate *N*-oxide; HBTU, *O*-(benzotriazol-1-yl)-1,1,3,3-tetramethyluronium hexafluorophosphate; HOBt, *N*-hydroxybenzotriazole; NMM, *N*-methylmorpholine; TFA, trifluoroacetic acid; TFE, 2,2,2-trifluoroethanol; TIS, triisopropylsilane.

* Corresponding author. Tel.: +39 089 969743; fax: +39 089 969702.
E-mail address: brunoin@unisa.it (I. Bruno).

0968-0896/$ - see front matter © 2010 Elsevier Ltd. All rights reserved.
doi:10.1016/j.bmc.2010.03.022

among others, apicidins,[7] FK228,[8] H-C toxin,[9] azumamides,[10] trapoxins[11] and chlamydocin.[12] The other chemical classes of HDACi[13] are carboxylates, benzamides, electrophilic ketones and hydroxamic acids like vorinostat (also known as SAHA)[14] which has been recently approved for treatment of cutaneous T-cell lymphoma. Encouraged by the interesting biological properties of FR235222, we decided first to undertake its total synthesis[15] and afterwards we moved our attention to explore some structure–activity relationships developing a first-generation of modified analogues whose biological behaviour was fully evaluated.[16] In the course of this biological screening we succeeded to identify a new hit, compound **2**, which showed an inhibition profile better than the parent molecule (Fig. 1). At the same time we invested many efforts in refining, at quantum mechanical level, the protein model represented by HDLP enzyme,[17] the bacterial homologue of human HDAC, in order to obtain more predictive affinity properties of the screened compounds. We then utilized this optimized model to dock the structures of the synthesized compounds in the binding pocket of the enzyme, and the collected data provided suggestions for new structural refinements of the tetrapeptide scaffold which should enhance affinity properties for the target.[18]

For example, the introduction of more than a bulky aromatic amino acid residue as tryptophan to the peptide backbone has shown to increase the ligand-enzyme complex stability, in addition, when these bulky residues were alternate in the sequence, an optimal interaction of the binders with the counterpart hydrophobic protein surface[18] was assured. Taking into account the computer aided suggestions we synthesized six new compounds **3**–**8** (Fig. 2), in which we also introduced more simplified Zn binding domains, in order to reduce the time of the synthetic procedures. In more details compounds **3**–**6** present, instead of the rare Ahoda (2*S*,9*R*-2-amino-9-hydroxy-8-oxodecanoic acid) residue joined to the cyclopeptide scaffold, a carboxylic acid functionalized spacer, identical to that present in the potent HDAC inhibitor Azumamide E[10] in contrast compounds **7** and **8**, possess the hydroxamic acid[19] functionality (Fig. 2) as Zn chelating element.

3. Docking studies

The X-ray structure of HDLP[17] was used as a macromolecule model in docking calculations, applying refined enzyme calculation parameters, as described in our previous study on cyclopeptidic HDAC inhibitors,[20] related to the electrostatic and van der Waals terms of binding energy. We also applied these protein parameters, previously optimized,[20] in a recent analysis on other HDAC bioactive tetrapeptide ligands[18,20] and on cyclopeptide mimetics,[21] reaching a good qualitative accordance between the results of theoretical K_D and biological assays.

In the molecular modelling calculations the carboxylic function of **3–6** was considered as dissociated at physiological pH and, consequently, deprotonated in the simulations.

Because AUTODOCK 3.0.5 software[22] does not allow rotations of the cyclic portion during the calculations, a preliminary conformational search was performed on structures **4**, **6** and **8** through Monte Carlo Multiple Minimum (MCMM) method,[23] to get the global minimum conformations of the putative ligands and to use these as starting points in the docking studies. In particular, the *cis*- and *trans*-isomers, around the peptide bond between proline and tryptophan, have been considered in the conformational search. Compounds **3** and **7** present the same tetrapeptide core of compound **2**, whose experimental structure has been previously determined.[18] A comparison of ^{1}H and 2D-NOESY spectra revealed an expected superimposition of the resonances, thus the structures of **3** and **7** were built from the experimental representative conformations of *cis*- and *trans*-isomers found for **2**.[18] The *cis*- and *trans*-isomers of **3**, **4** and **6–8** were analysed to evaluate if one or both isomers could be interacting with the biological target. In this section we will describe the detailed docking results for both isomers of compound **6**, as they gave the best calculated binding affinity (4.83×10^{-12} M^{-1} for *cis* and 8.65×10^{-12} M^{-1} for *trans*-isomer). The analysis of the theoretical results revealed that the *cis*- and *trans*-isomers of **6** showed an overlapped docked conformations in the binding site of HDLP (Fig. 3), establishing the same interactions with the macromolecular counterparts.

The side chain of tryptophan involved in the *cis*–*trans* isomerism was accommodated in a deep pocket delimited by the Q192, Y186, A197, F200, and K267 residues (Fig. 4), enveloping the indole ring and strongly contributing to the complex stability as found for **2**.[18]

Moreover, the NH group of the indole formed a hydrogen bond with the oxygen in the side chain of Q192, also showed by the docked structure of **2**.[18] The remainder aromatic group interacted with an opposite hydrophobic cavity of protein surface, formed by N20, H21, P22 and Y91 (Fig. 4) and it was hydrogen bonded with the side chains of H21 and Y91. The carboxylate moiety interacted with the catalytic portion of the enzyme coordinating the zinc ion in bidentate manner (Fig. 3) and established a hydrogen bond with $H^{\varepsilon 2}$ of H131, whereas the carbon chain formed van der Waals contacts with the 11 Å channel conducting to the zinc ion. The proline side chains pointed outside the protein, without giving any further interactions. Compound **4** is constituted by the same residues of **6**, except for the replacement of a tryptophan by a phenylalanine. Even though, the docking poses for *cis*- and *trans*-isomers of **4** and **6** showed the same spatial orientations in the binding site of HDLP (Fig. S2), the presence of a phenylalanine gave less extended van der Waals interactions with a consequent lower binding affinity for the protein. Compound **8** shared the same tetrapeptide core of **6**, indeed the common structural moiety followed closely the docked conformations of **6** *cis*- and *trans*-isomers in the binding site (Fig. S5), differing only for the coordination to the prosthetic group of the enzyme and for the carbon linker spatial orientation. The docked 3D arrangement of **5** is very similar to that calculated for **4**, **6** and **8** with the glycine instead of the proline (Fig. S3). In this

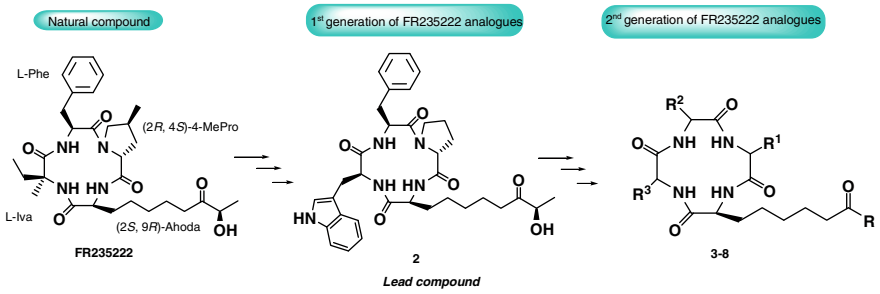

Figure 1. FR235222, **2** and second-generation analogues.

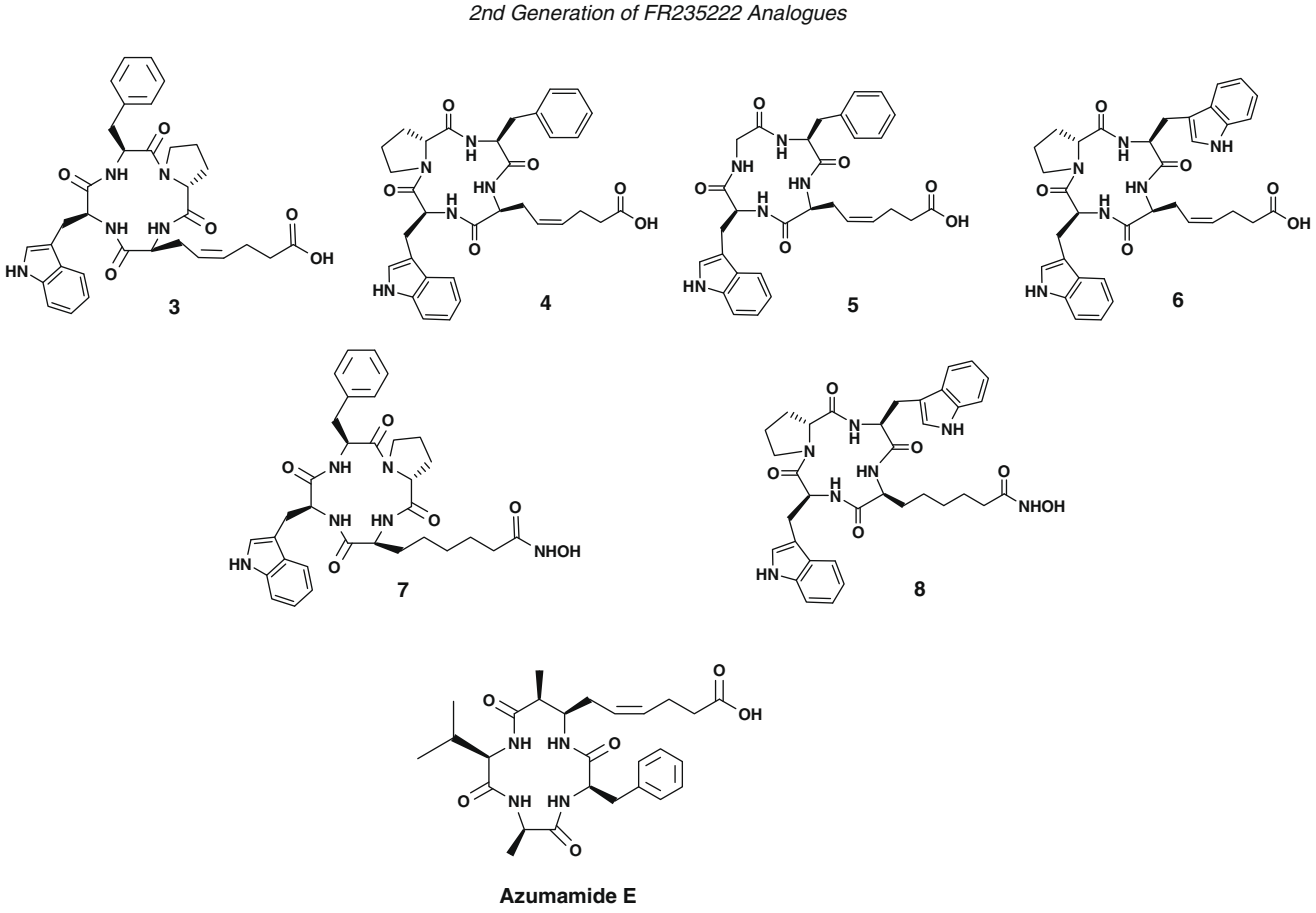

Figure 2. Chemical structures of analogues **3**–**8** and of Azumamide E.

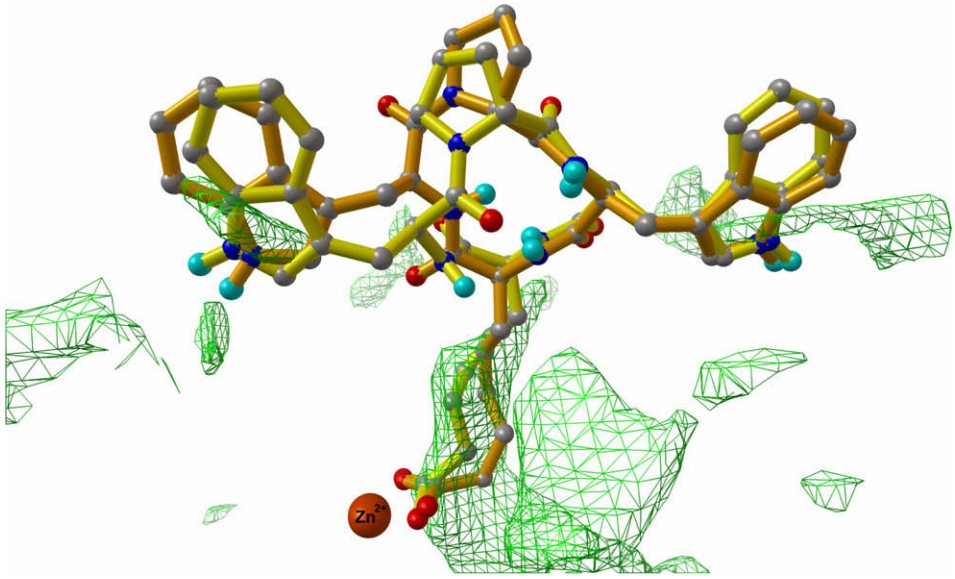

Figure 3. Superimposition of *cis*- and *trans*-isomers of **6** in the zinc-binding site. The green mesh represents the hydrophobic pocket of the protein. The Zn^{2+} is represented by a CPK sphere in red brick. The *cis*- and *trans*-isomers are depicted by sticks (respectively, orange and yellow) and balls (by atom type: C, gray; polar H, sky blue; N, blue; O, red). The figure highlights the similar interactions with the 11 Å deep hydrophobic channel of the esenoic carbon chain, and the close 3D arrangements of the proline and tryptophans residues on the receptor surface hydrophobic pockets.

case, also, the aromatic side chains were well accommodated into opposite hydrophobic hollows.

Compounds **3** and **7** structurally differed from **2** only for the linker and the metal binder. Thus, as expected, the calculated bioactive conformations were very similar to that found for their progenitor **2**.[18] In particular, for the *cis*-conformations of **3** and **7** the tryptophan side chain is accommodated in a deep hydrophobic cavity constituted by Q192, Y186, A197, F200, and K267, whereas

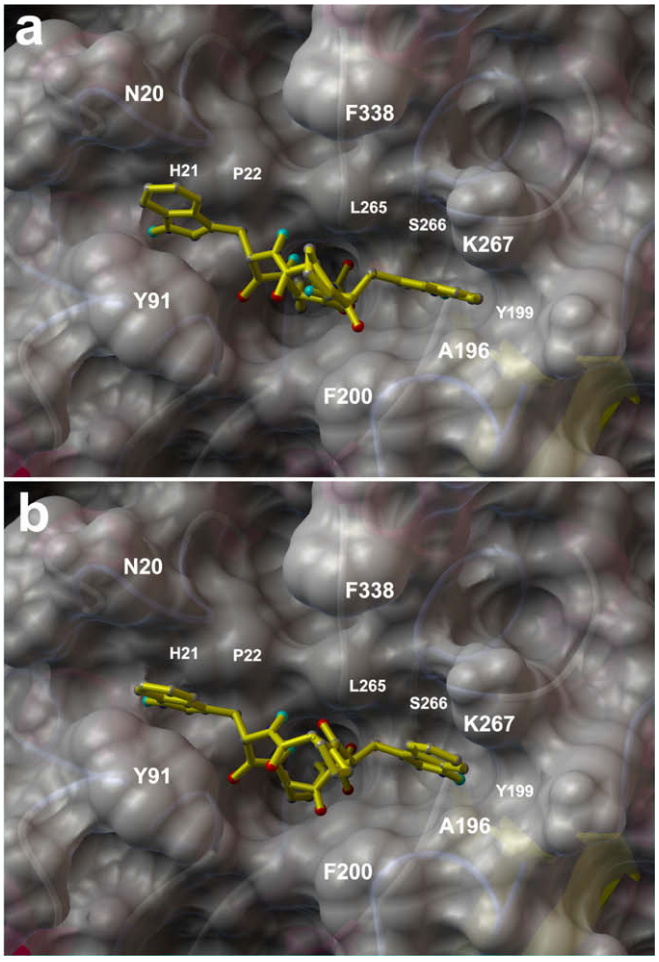

Figure 4. Three-dimensional models of the interactions formed by *cis*- and *trans*-isomers of **6** (respectively a, and b) with HDLP binding site. The protein is represented by molecular surface and ribbon. The ligands are depicted by sticks (yellow) and balls (coloured by atom type: C, gray; polar H, white; N, dark-blue; O, red). The figure highlights essential interactions: the side chains of tryptophans are located in hydrophobic pockets. The esenoic carbon chain establishes interactions with the 11 Å hydrophobic channel, with the zinc ion contained at the bottom and with amino acids of catalytic site.

the five-membered ring of proline was in contact with the side chains of Y91, E92 and G140 residues. The predicted bioactive conformations of the *trans*-isomers of **3** and **7**, was rotated by 180° respect to the docked *cis* conformations (Figs. S1 and S4) inverting the positions of tryptophan and proline into the surface cavities of the macromolecule.

Compared to compound **3** and **7**, structure **6** interacted with both aromatic side chains of tryptophan within the protein, increasing the affinity for the biological target. The same considerations could be made for **4**, **5** and **8**. Thus, the modification of the primary sequence of these new tetrapeptides seems to favour the interactions with the surface hydrophobic cavities of the enzyme. Moreover, the presence of bulky groups was important for the affinity to the macromolecule, because they increase the van der Waals contacts with the macromolecular counterparts, and the indole ring in all cases gave hydrogen bonds with the protein amino acids. Based on the obtained structure–activity relationships, we moved to the synthesis and biological evaluations of compounds **3–8**.

4. Chemistry

A convenient combination of both solid and solution phase synthetic approaches were used for the synthesis of the six analogues **3–8** (Scheme 1). Solid-phase synthesis of the linear peptide sequences, using standard *N*-Fmoc/^{t}Bu SPPS strategy, was performed on a 2-chlorotrityl chloride resin.[24] The solid support was loaded, under anhydrous conditions, with the first Fmoc-protected amino acid in presence of an excess of diisopropylethlyamine (DIEA) in DCM, followed capping of the unreacted trityl groups with methanol, according to general procedure **a** (see Section 7) (Scheme 1a). The obtained loading degree was determined by UV spectrophotometric analysis, using the general procedure **a'**. The resin was then submitted to coupling-deprotection cycles to build the linear protected peptides. For this purpose all the Fmoc-protected amino acids were activated by HOBt and HBTU in presence of *N*-methylmorpholine (NMM) or DIEA, as described in the general procedure **c**, and the progress of the amino acid coupling was checked through the Kaiser test. Fmoc deprotection, before each coupling step, was achieved by treatment of the resin-anchored peptide with a 20% solution of piperidine in *N*,*N*-dimethylformamide (DMF), according to general procedure **b**. To avoid the undesired diketopiperazine formation at the dipeptide level, as consequence of the presence of proline residue, during Fmoc removal in piperidine, we performed a fast Fmoc deprotection cycle at the level of the second coupling reaction (see Section 7). The next step consisted of Fmoc protecting group removal from the *N*-terminal residue, then the protected peptide was cleaved from the resin 2-ClTrt resin by using a 2:2:6 acetic acid/2,2,2-trifluoroethanol/dicholoromethane (AcOH/TFE/DCM) solvent mixture, according to procedure **d**. The linear tetrapeptides (**3a–8a**), obtained in high yields (88–95%), were cyclized, in DCM/DMF under highly dilute conditions with HATU as coupling reagent and DIEA, following general procedure **e**, to give the desired cyclopeptides (**3b–8b**) (Scheme 1a).

Removal of N^{in}-Boc protecting group was achieved using 95% aqueous trifluoroacetic acid (TFA), according to procedure **f**.

Finally the advanced precursors **3c–8c** were submitted to olefin cross-metathesis reactions either with 4-pentenoic acid **9**, to give the final compounds **3–6**, or with its hydroxamate derivative **10** (see Section 7) to give **7d–8d** (Scheme 1b). Metathesis reactions were carried out using microwave irradiation, in order to speed up the reaction rate.[25] As experienced in our previous studies, we used Grubbs' second-generation catalyst, which was found to be more stable to air and more reactive in our reaction conditions.[26] The optimal conditions found were: 18% mol of Grubbs' second-generation catalyst, DCM as the solvent and microwave heating at 300 W, 60 °C, for two 30 min periods (general procedure **g**). The reaction mixture was degassed with argon after the first 30 minutes to give off any dissolved ethene. The structures of the desired compounds **3–6** and **7d–8d** were confirmed by analytical RP-HPLC and mass spectrometry. Compounds **7d–8d** were subjected first to Trt groups deprotection by TFA (1% in DCM) and then to catalytic hydrogenation, yielding expected hydroxamate **7–8**, according to general procedure **h** and **i**.

The crude products were purified by semi-preparative RP-HPLC on a C18 column and the structures of **3–8** were confirmed by MS and NMR analysis.

5. Biological activity

To evaluate the potency and the selectivity of these compounds as HDAC inhibitors their activity on distinct HDAC isotypes was compared with that of the parent compound **2** (Table 1). The test system included class IIa-specific assays relying on the use of HDAC4, 5, and 7 catalytic domains purified to homogeneity from bacterial cells,[27,28] and on a class IIa-specific in vitro substrate.[27,29] This assay format makes it possible to measure the intrinsic catalytic activity of class IIa HDACs in the absence of contaminant endogenous class I members.

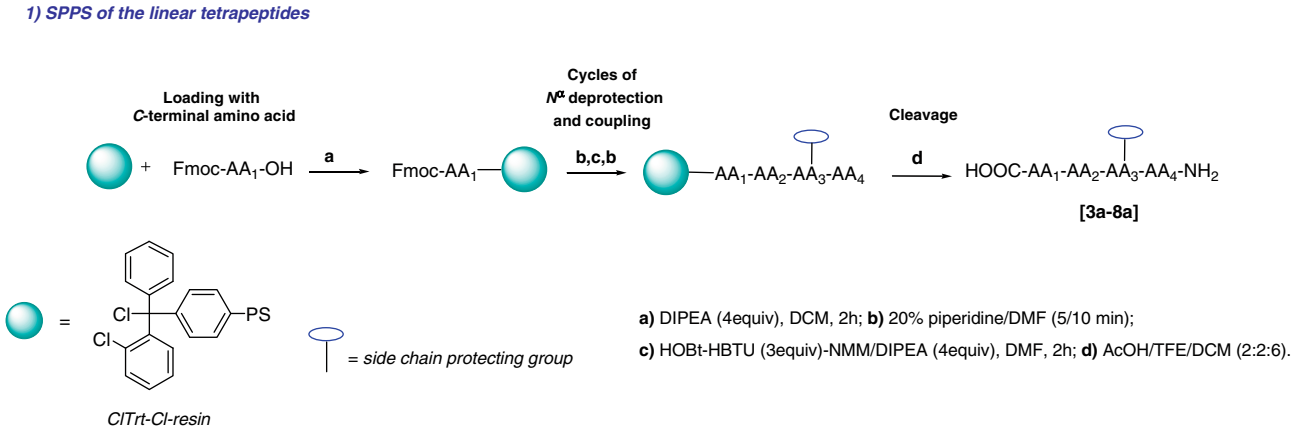

Scheme 1a. General synthetic approach for analogues **3c**–**8c**.

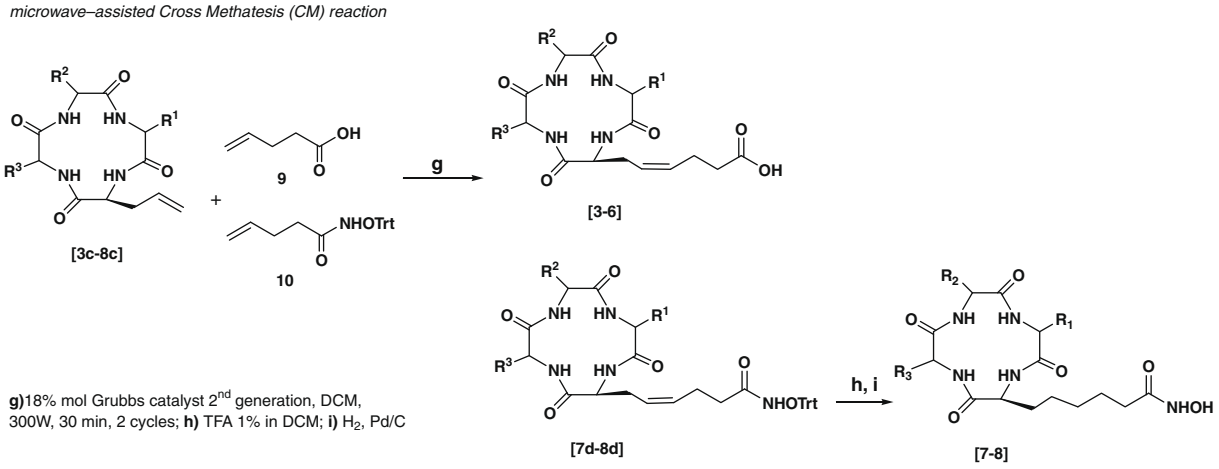

Scheme 1b. Synthetic strategy for compounds **3**–**8**.

Our reference compound **2** displayed submicromolar inhibitory activity on class I HDACs 1, 2, and 3. Its potency was similar to that measured on deacetylation reactions catalyzed by HDACs present in the nuclear extract (NE) from HeLa cells.

In contrast with molecular docking predictions, compounds **4** and **5** showed no measurable inhibitory activity to a concentration up to 50 μM on reactions catalyzed by the HeLa nuclear HDACs, while compound **6** showed only a weak activity at the same conditions. In contrast, **3** displayed a moderate, broad-spectrum HDAC inhibitor activity.

Compounds **7** and **8** showed a more restricted spectrum of activity than **3**, displaying a moderate propensity towards HDACs 4, 5, and 6, and a weak to undetectable activity on class I HDAC1, 2, 3. Compound **7** was also selective over HDAC8, therefore showing class II-specificity. Most of the well- known HDAC inhibitors either do not discriminate between class I and class II members, or are specific for class I HDACs. Class IIb HDACs 6 and 10 have been found to be resistant to cyclic peptide inhibitors such as trapoxin and CHAPS,[30,31] and to be selectively inhibited by non peptidic compounds.[32,33] Class IIa HDACs 4, 5, 7, 9 have been less extensively characterized in terms of inhibition profile. However recently described class IIa-specific inhibitors[34,35] do not include peptidic compounds.

6. Conclusion

In conclusion a small array of carboxy and hydroxamate derivatives of the known potent HDAC inhibitors FR235222 has been developed. In compounds **3–8** we modified both the composition of tetrapeptidic core and the functional linker, in order to expand the chemical diversity and to simplify the synthetic procedure. Unfortunately, even though molecular modelling studies showed that the peptidic scaffold efficiently fit with the protein counter-

Table 1
Biological activities on individual HDAC isoforms

Compound	HDAC subtype								
	HeLa NE	1	2	3	4	5	6	7	8
	IC_{50}[e] (μM)								
TSA	0.02 (0.009)								
2 (Lead)	0.133 (0.0057)	0.0675 (0.0021)	0.179 (0.030)	0.0247 (0.0004)	50% inh.[a] (4.7)	ND[b]	9.4 (0.65)	ND[b]	NA[c]
3	23.6 (2.1)	10.2 (2.65)	11.4 (4.53)	22 (1)	37% inh.[d] (2.83)	NA[c]	33.6 (5.5)	NA[c]	23 (0.88)
4	NA[c]								
5	NA[c]								
6	30% inh.[a] (6.2)								
7	ND[b]	42% inh.[d] (3.81)	30% inh.[d] (10.61)	14.7% inh.[d] (1.77)	9.6 (0.14)	31 (4.24)	2 (0.17)	NA[c]	NA[c]
8	ND[b]	73 (1)	34% inh.[a] (8.5)	23.5% inh.[a] (3.5)	10.65 (2.33)	31 (4.74)	24.7 (5.77)	48.5% inh.[a] (10.61)	27.6 (3.25)

[a] % inhibition at 100 μM.
[b] Not determined.
[c] Not active up to 50 μM.
[d] % inhibition at 50 μM.
[e] Values are means of 2–3 experiments. Standard deviations are in parenthesis.

part, the biological data are not very satisfactory, as the tested molecules showed only a moderate HDAC inhibition activity. Probably, the modification of the functional domain could be responsible of the activity decrease. However, we observed that variations in the amino acid composition of the peptidic core seem to affect the isoform profile, in fact compounds **7** and **8** displayed a major specificity towards class II HDAC enzymes. Even though the role played by each HDAC isotype in carcinogenesis still remains unclear, it is worthy to note that this kind of specificity has not previously reported in cyclopeptidic compounds.

7. Experimental section

7.1. General information

All chemicals were purchased from commercial sources and were used as received without further purification. Unless specified, solvents were reagent grade; they were purchased from Aldrich, Fluka, Carlo Erba. CH_2Cl_2 and DMF used for solid-phase reactions were synthesis grade (dried over activated molecular sieves (4 Å)). H_2O and CH_3CN were HPLC grade. 2-Chlorotrityl chloride resin (100–200 mesh), 1% DVB, (ClTrt-Cl, loading level: 1.4 $mmolg^{-1}$), Fmoc-D-Pro-OH, Fmoc-L-Phe-OH, Fmoc-L-Trp-(Boc)-OH, Fmoc-Gly-OH, Fmoc-L-AllylGly-OH, HOBt, and HBTU were purchased from Novabiochem and Neosystem. HATU, was purchased from Fluka.

Solid-phase peptide syntheses, using the Fmoc-*t*Bu strategy, were carried out on a polypropylene ISOLUTE SPE column on a VAC MASTERsystem, a manual parallel synthesis device purchased from Stepbio. All solid phase reactions were run under a nitrogen atmosphere with dry solvents. All cross-metathesis (CM) reactions were carried out under an argon atmosphere with dry, degassed solvents under anhydrous conditions. Grubbs catalyst second-generation was purchased from Aldrich.

For estimation of Fmoc amino acids on the resin, absorbance at λ = 301 nm was recorded on a Shimadzu UV 2101 PC.

Electrospray mass spectrometry (ES-MS) was performed on a LCQ DECA ThermoQuest (San Josè, California, USA) mass spectrometer. High resolution mass spectra (HRMS) were acquired on a Q-Tof ULTIMA (Waters, Manchester UK) calibrated with [Glu]-Fibrinopeptide B fragments using standard experimental conditions.

Analytical and semipreparative reversed-phase HPLC was performed on a Jupiter C_{18} column (250 × 4.60 mm, 5 μ, 300 Å, flow rate = 1 $mLmin^{-1}$; 250 × 10.00 mm, 10 μ, 300 Å, flow rate = 5 mL min^{-1}, respectively). The binary solvent system (A/B) was as follows: 0.1% TFA in water (A) and 0.1% TFA in CH_3CN (B). The absorbance was detected at 220–240 nm.

All microwave irradiation experiments were carried out in a dedicated CEM-Discover Focused Microwave Synthesis apparatus, operating with continuous irradiation power from 0 to 300 W utilizing the standard absorbance level of 300 W maximum power. The Discover™ system offers controllable ramp time, hold time (reaction time) and uniform stirring. The temperature was monitored using the CEM-Discover built-in-vertically-focused IR temperature sensor.

All NMR spectra (^{1}H, HMBC, HSQC, TOCSY, COSY, ROESY) were recorded on a Bruker Avance DRX600, at T = 298 K. Compounds **3**–**8** were dissolved in 0.5 mL DMSO-d_6 (99.95%, Carlo Erba, 99.95 atom% D) (^{1}H NMR δ = 2.50 ppm, ^{13}C NMR δ = 39.5 ppm). NMR data were processed on a Silicon Graphics Indigo 2 workstation using UXNMR software. Chemical shifts are expressed as δ (ppm) (see Supplementary data).

8. Computational details

All ligands were built and their geometries optimized through MacroModel 8.5 software[36] package and using the OPLS-AA force field.[37] For **4**, **6** and **8** both *cis* and *trans*-isomers, around the peptide bond formed by amine and carboxylic groups, respectively, of proline and tryptophan residues, were considered. Monte Carlo Multiple Minimum (MCMM) method of the MacroModel package[36] was used in order to allow a full exploration of the conformational space of **4**, **6** and **8** *cis* and *trans*-isomers, with a 50 kJ mol^{-1} upper energy limit and 10,000 steps. The so obtained geometries were optimized using the Polak–Ribier conjugate gradient algorithm (PRCG, 9×10^7 steps, maximum derivative less than 0.001 kcal/mol). A GB/SA (generalized Born/surface area)[38] solvent treatment was used, mimicking the presence of H_2O, in the geometry optimization and in the conformational search steps. The protein (1C3R.pdb)[17a] for the docking calculations was previously prepared[20] using MacroModel software: all hydrogen were added, bond order and missing atoms were checked by visual inspection, and the charges of side chains were assigned considering their pK_a. The structures of **3** and **7** presenting an overlapping ^{1}H proton and 2D-NOESY spectra with compound **2** reported in our previous studies of FR235222 analogues.[18] Thus, structures of **3** and **7** were built from the previously determined experimental structures of *cis*- and *trans*-isomers of **2**, leaving unaltered the found 3D arrangements of the common portions.

AUTODOCK 3.0.5[22] was used for all docking calculations. HDLP (histone deacetylase-like protein) is a metalloprotein, so a nonbonded model for metallic center according to the nonbonded Zn parameters of Stote and Karplus[39] (zinc radius = 1.10 Å, well depth = 0.25 kcal/mol) was used. In order to have an accurate

weight of the electrostatics, the previously derived partial charge of Zn = 1.175 and of the amino acids involved in the catalytic center (A169, H170, D168, D258), were used.[20] In particular the above charges were calculated at DFT theory level using the chelpg method.[40]

For all the docking calculations a grid box size of $66 \times 64 \times 64$ points spaced by 0.375 Å, centred between Zn^{2+} and H170 and covering the catalytic centre surface of HDLP was used. For all the docked structures, all bonds were treated as active torsional bonds except the amide bonds. In order to achieve a representative conformational space during the docking calculations, eleven calculations consisting of 256 runs were performed, obtaining 2816 structures (256×6). The Lamarckian genetic algorithm was used for dockings. An initial population of 600 randomly placed individuals, a maximum number of 5×10^6 energy evaluations, and a maximum number of 6×10^6 generations were taken into account. A mutation rate of 0.02 and a crossover rate of 0.8 were used, and the local search frequency was set up at 0.26.

Results differing by less than 2 Å in positional root-mean-square deviation (rmsd) were clustered together and represented by the result with the most favourable free energy of binding.

All the 3D models were depicted using the Phyton software:[41] molecular surfaces are rendered using Maximal Speed Molecular Surface (MSMS)[42] and, in Figure 3, the hydrophobic pocket of the protein is represented as an isocontour.[43]

8.1. General procedures for the synthesis of compound s 3–8

(**a**) *Loading of the resin*: The ClTrt-Cl resin was placed in a 25 mL polypropylene ISOSOLUTE syringe on a VAC MASTER system, swollen in 3 mL of DMF for 1 h, and then washed with 2×3 mL of DCM.

A solution of Fmoc-AA-OH (1.1 equiv) and DIEA (4 equiv) in 2.5 mL of dry DCM was added and the mixture was agitated for 2 h with a N_2 stream. The mixture was then removed, and the resin was washed with 3× DCM/MeOH/DIEA (17:2:1), and sequentially with the following washing/treatments: DCM 3×3 mL, DMF 2×3 mL, DCM 2×3 mL (1.5 min each).

(**a′**) *Estimation of the level of first residue attachment*: Resin loading was determined by UV quantification of the Fmoc-piperidine adduct.

The assay was performed on a duplicate samples: 0.4 mL of piperidine and 0.4 mL of DCM were added to two dried samples Fmoc amino acid-resin (~3.0 mg) in two volumetric flasks of 25 mL. The reaction was allowed to proceed for 30 min at rt and than 1.6 mL of MeOH were added and the solutions were diluted to 25 mL volume with DCM. A reference solution was prepared in a 25 mL volumetric flask using 0.4 mL of piperidine, 1.6 mL of MeOH and DCM to volume. The solutions were shaken and the absorbance of the samples versus the reference solution was measured at 301 nm. The substitution level (expressed in mmol of amino acid/g of resin) was calculated from the equation: mmol $g^{-1} = (A_{301}/7800) \times (25 \text{ mL g}^{-1}$ of resin). The obtained loading degree was: 0.28–0.40 mmol g^{-1}.

(**b**) *Fmoc deprotection*: 20% piperidine in DMF (3 mL, 1×1.5 min, 1×5 min or 1×10 min); washings in DMF 2×3 mL, DCM 2×3 mL, DMF 2×3 mL, (1.5 min each).

(**c**) *Peptide coupling conditions*: The coupling reaction was promoted by a HOBt/HBTU in DMF coupling protocol: Fmoc-amino acid, (3–4 equiv), HOBt (3–4 equiv), HBTU (3–4 equiv) and NMM (4–5 equiv) or DIEA (4–5 equiv) were agitated under N_2 in 2.5 mL of DMF for 2 h. After each coupling, washings were carried out with DMF (3 mL, 3×1.5 min), and DCM (3 mL, 3×1.5 min).

(**d**) *Cleavage*: The dried peptide resin was treated for 2 h, under stirring, with the following cleavage mixture: AcOH/TFE/DCM (2:2:6; 10 μL × 1 mg of resin). Then the resin was filtered off and washed with neat cleavage mixture (3 mL, 3×1.5 min). After addition of hexane (15 times volume) to remove acetic acid as an azeotrope, the filtrate was concentrated and lyophilized (83–95% overall yield).

(**e**) *Cyclization*: The cyclization step was performed in solution at a concentration of 7.8×10^{-5} M with HATU (2.0 equiv) and DIEA (2.5 equiv) in DCM/DMF.[44] The solution was stirred at 4 °C for 1 h and then allowed to warm to room temperature for 1 h. The cyclization reaction was monitored via HPLC and ES-MS spectra. After 2 h the solvent was removed under reduced pressure.

Compound **3b**: A portion of the linear peptide (71.8 mg, 0.11 mmol) was dissolved in DCM/DMF (1410 mL/800 μL) with HATU (83.6 mg, 0.22 mmol, 2.0 equiv) and DIEA (47.0 μL, 0.27 mmol, 2.5 equiv).

RP HPLC: Jupiter C-18 column (250×4.60 mm, 5 μ, 300 Å), from 5% B to 100% B over 30 min, flow rate of 1 mL/min, $\lambda = 220$ nm. t_R 22.7 min; ES-MS: m/z 628.4 $[M+H]^+$, 650.4 $[M+Na]^+$.

Compound **4b**: A portion of the linear peptide (61.4 mg, 0.09 mmol) was dissolved in DCM/DMF (1153 mL/730 μL) with HATU (68.4 mg, 0.18 mmol, 2.0 equiv) and DIEA (38.3 μL, 0.22 mmol, 2.5 equiv).

RP HPLC: Jupiter C-18 column (250×4.60 mm, 5 μ, 300 Å), from 5% B to 100% B over 30 min, flow rate of 1 mL/min, $\lambda = 240$ nm. t_R 26.6 min; ES-MS: m/z 628.3 $[M+H]^+$.

Compound **5b**: A portion of the linear peptide (92.5 mg, 0.15 mmol) was dissolved in DCM/DMF (1923 mL/1.0 mL) with HATU (114.1 mg, 0.30 mmol, 2.0 equiv) and DIEA (65.3 μL, 0.37 mmol, 2.5 equiv).

RP HPLC: Jupiter C-18 column (250×4.60 mm, 5 μ, 300 Å), from 5% B to 100% B over 30 min, flow rate of 1 mL/min, $\lambda = 220$ nm. t_R 22.6 min; ES-MS: m/z 588.0 $[M+H]^+$, 610.2 $[M+Na]^+$.

Compound **6b**: A portion of the linear peptide (70.4 mg, 0.09 mmol) was dissolved in DCM/DMF (1152 mL/700 μL) with HATU (68.4 mg, 0.18 mmol, 2.0 equiv) and DIEA (38.3 μL, 0.22 mmol, 2.5 equiv).

RP HPLC: Jupiter C-18 column (250×4.60 mm, 5 μ, 300 Å), from 5% B to 100% B over 30 min, flow rate of 1 mL/min, $\lambda = 220$ nm. t_R 27.2 min; ES-MS: m/z 767.2 $[M+H]^+$, 789.0 $[M+Na]^+$.

Compound **7b**: A portion of the linear peptide (62.8 mg, 0.09 mmol) was dissolved in DCM/DMF (1153 mL/700 μL) with HATU (68.4 mg, 0.18 mmol, 2.0 equiv) and DIEA (38.3 μL, 0.22 mmol, 2.5 equiv).

RP HPLC: Jupiter C-18 column (250×4.60 mm, 5 μ, 300 Å), from 5% B to 100% B over 30 min, flow rate of 1 mL/min, $\lambda = 220$ nm. t_R 22.6 min; ES-MS: m/z 628.4 $[M+H]^+$, 650.4 $[M+Na]^+$.

Compound **8b**: A portion of the linear peptide (63.0 mg, 0.08 mmol) was dissolved in DCM/DMF (1025 mL/500 μL) with HATU (60.4 mg, 0.16 mmol, 2.0 equiv) and DIEA (34.8 μL, 0.20 mmol, 2.5 equiv).

RP HPLC: Jupiter C-18 column (250×4.60 mm, 5 μ, 300 Å), from 5% B to 100% B over 30 min, flow rate of 1 mL/min, $\lambda = 220$ nm. t_R 27.1 min; ES-MS: m/z 767.2 $[M+H]^+$, 789.4 $[M+Na]^+$.

(**f**) *Boc deprotection*: Side-chain deprotection was carried out by treatment with TFA/H_2O/TIS (95:4:1, 10 ml × 1 mg) for 20 min while stirring.

The crude product was purified by semipreparative RP HPLC on a Jupiter C-18 column (250×10.00 mm, 10 μ, 300 Å).

Compound **3c**: from 5% B to 100% B over 40 min, flow rate of 5 mL/min, $\lambda = 240$ nm. t_R 20.0 min; ES-MS: m/z 528.3 $[M+H]^+$, 550.4 $[M+Na]^+$.

Compound **4c**: from 5% B to 100% B over 30 min, flow rate of 5 mL/min, $\lambda = 220$ nm. t_R 21.1 min; ES-MS: m/z 528.1 $[M+H]^+$.

Compound **5c**: from 5% B to 100% B over 50 min, flow rate of 5 mL/min, $\lambda = 220$ nm. t_R 21.4 min; ES-MS: m/z 488.2 $[M+H]^+$.

Compound **6c**: from 5% B to 100% B over 50 min, flow rate of 5 mL/min, $\lambda = 240$ nm. t_R 21.8 min; ES-MS: m/z 567.3 $[M+H]^+$.

Table 2
Calculated and observed molecular weights (by MS and HPLC analysis) and HPLC t_R data for compounds **3**–**8**

Compound	Formula	ES-MS $[M+H]^+$		HRMS		HPLC
		Calcd	Found	Calcd for $[M+H]^+$	Found	t_R (min)
3	$C_{33}H_{37}N_5O_6$	599.6	600.2	600.2822	600.2902	33.57[a]
4	$C_{33}H_{37}N_5O_6$	599.6	600.1	600.2822	600.2902	35.31[b]
5	$C_{30}H_{33}N_5O_6$	559.6	560.2	560.2509	560.2404	33.50[c]
6	$C_{35}H_{38}N_6O_6$	638.7	639.3	639.2931	639.2824	32.89[d]
7	$C_{33}H_{40}N_6O_6$	616.7	617.2	617.3088	617.2998	26.20[e]
8	$C_{35}H_{41}N_7O_6$	655.7	656.4	656.3197	656.2999	30.90[f]

The binary solvent system (A/B) was as follows: 0.1% TFA in water (A) and 0.1% TFA in acetonitrile (B).
[a] 5–65% of solvent system (A/B) for 70 min.
[b] 5–60% of solvent system (A/B) for 70 min.
[c] 5–55% of solvent system (A/B) for 60 min.
[d] 5–70% of solvent system (A/B) for 75 min.
[e] 5–100% of solvent system (A/B) for 30 min.
[f] 5–100% of solvent system (A/B) for 95 min.

Compound **7c**: from 5% B to 100% B over 40 min, flow rate of 5 mL/min, λ = 240 nm. t_R 19.8 min; ES-MS: *m*/*z* 528.3 $[M+H]^+$, 550.4 $[M+Na]^+$.

Compound **8c**: from 5% B to 100% B over 50 min, flow rate of 5 mL/min, λ = 240 nm. t_R 21.8 min; ES-MS: *m*/*z* 567.3 $[M+H]^+$, 589.0 $[M+Na]^+$.

(**g**) *Optimized microwave cross-metathesis reactions*: The olefins (1.1–1.2 equiv) were stirred in dry DCM (0.19 M) in a microwave vial. Grubb's second-generation catalyst (18 mol %) was added, and the mixture stirred and subjected to microwave radiation, 300 W, 80 °C, for 30 min. The reaction mixture was then degassed with argon for 2 min and mixture stirred and subjected to MW radiation for a further 30 min at the same conditions. After the irradiation period, the reaction vessel was cooled rapidly (60–120 s) to ambient temperature by air jet cooling. The mixture was dried and then purified by HPLC chromatography.

(**h**) *Trt deproptection*: Removal of trytil group was performed in solution with TFA/TIS/DCM (1:1:98) for 30 min under stirring.

(**i**) *Catalytic hydrogenation*: To the cyclopeptides dissolved in MeOH, 10% Pd–C was added and the mixture was stirred under hydrogen atmosphere overnight. The reaction was monitored by TLC, HPLC and ESMS. After completion of the reaction, the catalyst was filtered off and MeOH was evaporated.

The crude products were purified by semipreparative reverse phase HPLC (on a Jupiter C-18 column: 250 × 10.00 mm, 10 μ, 300 Å, flow rate = 5 mL/min) using the gradient condition reported in Table 2 and characterized by ES-MS, HRMS, and NMR spectra.

8.2. Synthesis of compound 10

To a stirred solution of 4-pentenoic acid **9** (150 mg, 1.50 mmol, 153.3 μL) in DMF (1.36 mL) were added *O*-trytilhydroxylamine hydrochloride (413 mg, 1.50 mmol), HOBt (229,65 mg, 1.50 mmol), DIC (232,26 μL, 1.50 mmol) and DIEA (1.50 mmol, 261.18 μL), at 0 °C. After stirring at room temperature for 1 h, the reaction mixture was evaporated. The reaction was monitored by HPLC and ESMS. After completion of the reaction, the crude product was purified by semipreparative reverse phase HPLC (on a Jupiter C-18 column: 250 × 10.00 mm, 10 μ, 300 Å, flow rate = 5 mL/min) using the following gradient: 15–100% of solvent system (A/B) for 60 min; t_R (min) 33.0; ESI-MS: *m*/*z* = 357.1, $[M+H]^+$, white solid (56% yield calculated after HPLC purification).

8.3. Biological assays

HeLa nuclear extract was prepared as described.[45] Full-length HDAC1, 2, 3, 6 were purified from transiently transfected HEK293 cell extracts as previously described.[27] HDAC4, 5, 7 catalytic domains were expressed and purified from *Escherichia coli* as described.[27,28] Full-length HDAC8 was purified from *E. coli* soluble extracts as described.[46] IC_{50} values were determined using the HDAC fluorescent activity assay (BIOMOL Research Laboratories, Plymouth Meeting, PA). Assays were performed in 96-well plates according to the manufacturer's instructions by using either the commercial Fluor de Lys substrates KI-104 (HDAC1, 2, 3, 6) and KI-178 (HDAC8), or the trifluoro acetyl lysine substrate (HDAC4, 5, 7).[27] HDACi activities were evaluated by pre-incubating compounds and recombinant enzymes in assay buffer at rt for 15 min, before substrate addition. Mean values of at least two independent assays are reported. Standard deviation values were <20%.

Acknowledgements

Financial support by the University of Salerno, MIUR (Rome) and PRIN-06 are gratefully acknowledged. We also thank to C. Paolini e M.C. Nardi for technical support.

Supplementary data

Supplementary data associated with this article can be found, in the online version, at doi:10.1016/j.bmc.2010.03.022.

References and notes

1. (a) Hadnagy, A.; Beaulieu, R.; Balicki, D. *Mol. Cancer Ther.* **2008**, *7*, 740; (b) Biel, M.; Wascholowski, V.; Giannis, A. *Angew. Chem., Int. Ed.* **2005**, *44*, 3186; (c) Marks, P. A.; Miller, T.; Richon, V. M. *Curr. Opin. Pharmacol.* **2003**, *3*, 344.
2. (a) Paris, M.; Porcelloni, M.; Fattori, D. *J. Med. Chem.* **2008**, *51*, 1505; (b) Bieliauskas, A. V.; Pflum, M. K. H. *Chem. Soc. Rev.* **2008**, *37*, 1402; (c) Gallinari, P.; Di Marco, S.; Jones, P.; Pallaoro, M.; Steinkuhler, C. *Cell Res.* **2007**, *17*, 195.
3. (a) Acharya, M. R.; Sparreboom, A.; Venitz, J.; Figg, W. D. *Mol. Pharmacol.* **2005**, *68*, 917; (b) Monneret, C. *Eur. J. Med. Chem.* **2005**, *40*, 1; (c) Minucci, S.; Pelicci, P. G. *Nat. Rev. Cancer* **2006**, *6*, 38; (d) Villar-Garea, A.; Esteller, M. *Int. J. Cancer* **2004**, *112*, 171; (e) Dokmanovic, M.; Clarke, C.; Marks, P. A. *Mol. Cancer Res.* **2007**, *5*, 981; (f) Pan, L.; Lu, J.; Huang, B. *Cell Mol. Immunol.* **2007**, *4*, 337; (g) Bolden, J. E.; Peart, M. J.; Johnstone, R. W. *Nat. Rev. Drug Disc.* **2006**, *5*, 769.
4. Witt, O.; Deubzer, H. E.; Milde, T.; Oehme, I. *Cancer Lett.* **2009**, *277*, 8.
5. de Ruijter, A. J.; van Gennip, A. H.; Caron, H. N.; Kemp, S.; van Kuilenburg, A. B. *Biochem. J.* **2003**, *370*, 737.
6. (a) Mori, H.; Urano, Y.; Kinoshita, T.; Yoshimura, S.; Takase, S.; Hino, M. *J. Antibiot.* **2003**, *56*, 181; (b) Mori, H.; Abe, F.; Furukawa, S.; Sakai, F.; Hino, M.; Fujii, T. *J. Antibiot.* **2003**, *56*, 80; (c) Mori, H.; Urano, Y.; Abe, F.; Furukawa, S.; Tsurumi, Y.; Sakamoto, K.; Hashimoto, M.; Takase, S.; Hino, M.; Fujii, T. *J. Antibiot.* **2003**, *56*, 72.
7. (a) Darkin-Rattray, S. J.; Gurnett, A. M.; Myers, R. W.; Dulski, P. M.; Crumley, T. M.; Allocco, J. J.; Cannova, C.; Meinke, P. T.; Colletti, S. L.; Bednarek, M. A.; Singh, S. B.; Goetz, M. A.; Dombrowski, A. W.; Polishook, J. D.; Schmatz, D. M. *Proc. Natl. Acad. Sci. U.S.A.* **1996**, *93*, 13143; (b) Singh, S. B.; Zink, D. L.; Liesch, J. M.; Mosley, R. T.; Dombrowski, A. W.; Bills, G. F.; Darkin-Rattray, S. J.; Schmatz, D. M.; Goetz, M. A. *J. Org. Chem.* **2002**, *67*, 815; (c) Han, J. W.; Ahn, S. H.; Park, S. H.; Wang, S. Y.; Bae, G. U.; Seo, D. W.; Known, H. K.; Hong, S.; Lee, Y. W.; Lee, H. W. *Cancer Res.* **2000**, *60*, 6068.

8. (a) Ueda, H.; Nakajima, H.; Hori, Y.; Fujita, T.; Nishimura, M.; Goto, T.; Okuhara, M. *J. Antibiot.* **1994**, *47*, 301; (b) Ueda, H.; Manda, T.; Matsumoto, S.; Mukumoto, S.; Nishigaki, F.; Kawamura, I.; Shimomura, K. *J. Antibiot.* **1994**, *47*, 315; (c) Furumai, R.; Matsuyama, A.; Kobashi, M.; Lee, K.-H.; Nishiyama, M.; Nakajima, H.; Tanaka, A.; Komatsu, Y.; Nishino, N.; Yoshida, M.; Horinouchi, S. *Cancer Res.* **2002**, *62*, 4916.
9. Walton, J. D. *Phytochemistry* **2006**, *67*, 1406.
10. Nakao, Y.; Yoshida, S.; Matsunaga, S.; Shindoh, N.; Terada, Y.; Nagai, K.; Yamashita, J. K.; Ganesan, A.; van Soest, R. W. M.; Fusetani, N. *Angew. Chem., Int. Ed.* **2006**, *45*, 7553.
11. Kijima, M.; Yoshida, M.; Suguta, K.; Horinouchi, S.; Beppu, T. *J. Biol. Chem.* **1993**, *268*, 22429.
12. Closse, A.; Huguenin, R. *Helv. Chim. Acta* **1974**, *57*, 545.
13. Paris, M.; Porcelloni, M.; Binaschi, M.; Fattori, D. *J. Med. Chem.* **2008**, *51*, 1505.
14. Grant, S.; Easley, C.; Kirkpatrik, P. *Nat. Rev. Drug Disc.* **2007**, *6*, 21.
15. Rodriquez, M.; Terracciano, S.; Cini, E.; Settembrini, G.; Bruno, I.; Bifulco, G.; Taddei, M.; Gomez-Paloma, L. *Angew.Chem.* **2006**, *118*, 437; *Angew. Chem., Int. Ed.* **2006**, *45*, 423.
16. Gomez-Paloma, L.; Bruno, I.; Cini, E.; Khochbin, S.; Rodriquez, M.; Taddei, M.; Terracciano, S.; Sadoul, K. *ChemMedChem* **2007**, *2*, 1511.
17. (a) Finnin, M. S.; Donigian, J. R.; Cohen, A.; Richon, V. M.; Rifkind, R. A.; Marks, P. A.; Breslow, R.; Pavletich, N. P. *Nature* **1999**, *401*, 188; (b) Wang, D.-F.; Wiest, O.; Helquist, P.; Lan-Hargest, H.-Y.; Wiech, N. L. *J. Med. Chem.* **2004**, *47*, 3409.
18. Di Micco, S.; Terracciano, S.; Bruno, I.; Rodriquez, M.; Riccio, R.; Taddei, M.; Bifulco, G. *Bioorg. Med. Chem.* **2008**, *16*, 8635.
19. Miller, T. A.; Witter, D. J.; Belvedere, S. *J. Med. Chem.* **2003**, *46*, 5097.
20. Maulucci, N.; Chini, M. G.; Di Micco, S.; Izzo, I.; Cafaro, E.; Russo, A.; Gallinari, P.; Paolini, C.; Nardi, M. C.; Casapullo, A.; Riccio, R.; Bifulco, G.; De Riccardis, F. *J. Am. Chem. Soc.* **2007**, *129*, 3007.
21. Pirali, T.; Faccio, V.; Mossetti, R.; Grolla, A. A.; Di Micco, S.; Bifulco, G.; Genazzani, A. A.; Tron. G. C. *Mol. Diversity* **2010**, *14*, 109.
22. Morris, G. M.; Goodsell, D. S.; Halliday, R. S.; Huey, R.; Hart, W. E.; Belew, R. K.; Olson, A. J. *J. Comput. Chem.* **1998**, *19*, 1639.
23. Chang, G.; Guida, W. C.; Still, W. C. *J. Am. Chem. Soc.* **1989**, *111*, 4379.
24. Barlos, K. et al *Tetrahedron Lett.* **1989**, *30*, 3947.
25. (a) Poulsen, S. A.; Bornaghi, L. F. *Tetrahedron Lett.* **2005**, *46*, 7389; (b) Chatterjee, A. K.; Choi, T.-L.; Sanders, D. P.; Grubbs, R. H. *J. Am. Chem. Soc.* **2003**, *125*, 11360.
26. Grubbs, R. H.; Lee, C. W.; Ding, S.; Scholl, M. *Org. Lett.* **1999**, *1*, 953.
27. Lahm, A.; Paolini, C.; Pallaoro, M.; Nardi, M. C.; Jones, P.; Neddermann, P.; Sambucini, S.; Bottomley, M. J.; Lo Surdo, P.; Carfí, A.; Koch, U.; De Francesco, R.; Steinkühler, C.; Gallinari, P. *Proc. Natl. Acad. Sci. U.S.A.* **2007**, *104*, 17335.
28. Bottomley, M. J.; Lo Surdo, P.; Di Giovine, P.; Cirillo, A.; Scarpelli, R.; Ferrigno, F.; Jones, P.; Neddermann, P.; De Francesco, R.; Steinkühler, C.; Gallinari, P.; Carfí, A. *J. Biol. Chem.* **2008**, *283*, 26694.
29. Jones, P.; Altamura, S.; De Francesco, R.; Gallinari, P.; Lahm, A.; Neddermann, P.; Rowley, M.; Serafini, S.; Steinkühler, C. *Bioorg. Med. Chem. Lett.* **2008**, *18*, 1814.
30. Fumurai, R.; Komatsu, Y.; Nishino, N.; Khochbin, S.; Yoshida, M.; Horinouchi, S. *Proc. Natl. Acad. Sci. U.S.A.* **2001**, *98*, 87.
31. Guardiola, A. R.; Yao, T.-P. *J. Biol. Chem.* **2002**, *277*, 3350.
32. Haggarty, S. J.; Koeller, K. M.; Wong, J. C.; Grozinger, C. M.; Schreiber, S. L. *Proc. Natl. Acad. Sci. U.S.A.* **2003**, *100*, 4389.
33. Itoh, Y.; Suzuki, T.; Kouketsu, A.; Suzuki, N.; Maeda, S.; Yoshida, M.; Nakagawa Miyata, H. N. *J. Med. Chem.* **2007**, *50*, 5425.
34. Mai, A.; Massa, S.; Pezzi, R.; Simeoni, S.; Rotili, D.; Nebbioso, A.; Scognamiglio, A.; Altucci, L.; Loidl, P.; Brosch, G. *J. Med. Chem.* **2005**, *48*, 3344.
35. Muraglia, E.; Altamura, S.; Branca, D.; Cecchetti, O.; Ferrigno, F.; Orsale, M. V.; Palumbi, M. C.; Rowley, M.; Scarpelli, R.; Steinkühler, C.; Jones, P. *Bioorg. Med. Chem. Lett.* **2008**, *18*, 6083.
36. MacroModel, version 8.5, Schrödinger LLC, New York, NY, 2003.
37. Jorgensen, W. L.; Maxwell, D. S.; Tirado-Rives, J. *J. Am. Chem. Soc.* **1996**, *118*, 11225.
38. Still, W. C.; Tempczyk, A.; Hawley, R. C.; Hendrickson, T. *J. Am. Chem. Soc.* **1990**, *112*, 6127.
39. Stote, R. H.; Karplus, M. *Proteins* **1995**, *23*, 12.
40. Breneman, C. M.; Wiberg, K. B. *J. Comput. Chem.* **1990**, *11*, 361.
41. Sanner, M. F. *J. Mol. Graphics Modell.* **1999**, *17*, 57.
42. Sanner, M. F.; Olson, A. J.; Spehner, J. C. *Biopolymers* **1996**, *38*, 305.
43. Bajaj, C.; Pascucci, V.; Schikore, D. In Fast IsoContouring for Improved Interactivity, Proceedings of ACM Siggrapf/IEEE Symposium on Volume Visualization, ACM Press, 1996; pp 39–46.
44. Terracciano, S.; Bruno, I.; Bifulco, G.; Avallone, E.; Smith, C. D.; Gomez-Paloma, L.; Riccio, R. *Bioorg. Med. Chem.* **2005**, *13*, 5225.
45. Nare, B.; Allocco, J. J.; Kuningas, R.; Galuska, S.; Myers, R. W.; Bednarek, M. A.; Schmatz, D. M. *Anal. Biochem.* **1999**, *267*, 390.
46. Vannini, A.; Volpari, C.; Filocamo, G.; Casavola, E. C.; Mirko Brunetti, M.; Renzoni, D.; Chakravarty, P.; Paolini, P.; De Francesco, R.; Gallinari, P.; Steinkühler, C.; Di Marco, S. *Proc. Natl. Acad. Sci. U.S.A.* **2004**, *101*, 15064.